Understanding the spread of typhoid fever: Combining vaccination and sanitation methods for better public health policies

Cite as: AIP Advances 14, 045227 (2024); doi: 10.1063/5.0201916
Submitted: 1 February 2024 • Accepted: 24 March 2024 •
Published Online: 15 April 2024

Alhassan Ibrahim,[1,2] Usa Wannasingha Humphries,[1,a)] Ibrahim Mohammed,[3,4] and Rahat Zarin[1]

AFFILIATIONS

[1] Department of Mathematics, Faculty of Science, King Mongkut's University of Technology, Thonburi (KMUTT), 126 Pracha Uthit Road, Bang Mod, Thrung Khru, Bangkok 10140, Thailand
[2] School of Continuing Education, Bayero University, Kano, Nigeria
[3] Department of Mathematical and Statistics, University of Strathclyde, Glasgow, United Kingdom
[4] Department of Mathematical Sciences, Abubakar Tafawa Balewa University, Bauchi, Nigeria

[a)] **Author to whom correspondence should be addressed:** usa.wan@kmutt.ac.th

ABSTRACT

Typhoid fever remains a major public health concern, affecting over nine million individuals globally each year. Mathematical modeling approaches can provide valuable insights into typhoid transmission dynamics and inform preventive strategies. In this study, we developed a compartmental model incorporating key features of typhoid epidemiology and two crucial interventions: vaccination and sanitation practices. The model stratifies the population into susceptible, vaccinated, exposed, asymptomatic infected, symptomatic infected, and recovered compartments and tracks the bacterial load in the environment. We established a disease-free equilibrium and basic reproduction number R_0. We also identified the endemic equilibrium and analyzed its existence. Numerical simulations demonstrated the critical impact of enhanced sanitation and vaccination in curtailing infections. Our model underscores the need for multifaceted control measures that encompass vaccine coverage, sanitation enforcement, and healthcare capacity building to mitigate typhoid in high-risk regions. This study provides a comprehensive framework to model the intricate transmission dynamics of typhoid fever, supporting informed public health policies and decision-making.

I. INTRODUCTION

Typhoid fever, an infectious bacterial disease, is primarily caused by *Salmonella typhi*.[1] This disease, commonly referred to as typhoid, poses a significant threat to public health globally. In 2019, it afflicted over 9×10^6 individuals and tragically claimed the lives of over 110 000 people.[2] This disease remains highly contagious, contributing to its persistent prevalence in various regions of the world. Notably, typhoid has established an endemic presence in many parts of the world, particularly in sub-Saharan Africa and Southeast Asia.[3,4]

The clinical manifestation of typhoid fever unfolds gradually; typically, manifestation of symptoms takes 1–3 weeks post-infection with *Salmonella typhi* bacteria.[5] These dangerous symptoms of typhoid are marked by a distressing onset, such as headaches, cough, and abdominal pain, creating a significant burden on the infected individual.[6] Concurrently, disturbances in the digestive system, including constipation and diarrhea, further worsen the overall condition.[6] Swift initiation of treatment, primarily through the administration of antibiotics, such as ampicillin, chloramphenicol, trimethoprim–sulfamethoxazole, and amoxicillin, facilitates rapid improvement in symptoms within 3–5 days.[7] However, the consequences of untreated typhoid are dire, leading to disease progression and severe outcomes, including potential fatality. Without timely intervention, typhoid can evolve into a life-threatening condition, underscoring the importance of early diagnosis and effective medical intervention. It is noteworthy that the most vulnerable demographic, with the highest reported case fatality rates, comprises children under the age of 4.[2]

Salmonella typhi propagates through the fecal–oral route, disseminating from infected individuals, whether symptomatic or asymptomatic. The primary mode of transmission involves contact with contaminated food and water sources, highlighting the critical role of environmental factors in the spread of pathogens. Notably, individuals harboring active typhoid infections, even those who display no apparent symptoms (asymptomatic), can excrete the bacteria in their feces, further perpetuating contamination of the surroundings.

The effective prevention of typhoid fever depends on a multifaceted approach that connects sanitation, hygiene practices, and vaccination strategies. Although maintaining robust sanitation and hygiene standards plays a pivotal role in minimizing the transmission of *Salmonella typhi*, vaccination has emerged as the most significant and direct preventive measure. Notably, two widely utilized vaccines have demonstrated efficacy in preventing typhoid outbreaks: the oral Vivotif, produced by Crucell, and the injectable Typhim Vi and Typherix, manufactured by Sanofi Pasteur and GlaxoSmithKline, respectively. These vaccines serve as crucial components of public health initiatives aimed at curtailing the incidence of typhoid fever, particularly in regions with heightened susceptibility. To ensure sustained immunity, recommended booster doses are integral, with oral vaccination schedules advising boosts every five years and injectable counterparts advocating for revaccination every two years.[8]

Numerous mathematical modeling studies have been conducted to demonstrate the complicated transmission dynamics of typhoid fever, reflecting a collective effort to enhance our understanding of this infectious disease.[9–12] Peter *et al.*[12] devised a comprehensive model encompassing the direct and indirect transmission dynamics of typhoid fever. Their study incorporated three key control interventions: educational campaigns, sanitation practices, and screening, along with early treatment. However, a notable limitation of their model was the omission of vaccination, a key preventive measure against typhoid, which raised concerns about the completeness of the proposed interventions.

In a parallel manner, Abboubakar and Racke in Ref. 9 developed a mathematical model that considered the transmission dynamics of typhoid fever within human populations. Their model included the following factors: the incubation period, utilization of imperfect vaccines, and influence of protective measures, such as environmental sanitation and treatment. In contrast to the work of Peter *et al.*, Abboubakar and Racke did not include the rare occurrence of person-to-person transmission, which acknowledges the multifaceted nature of typhoid transmission, paving the way for a more holistic assessment of control strategies.

Furthermore, Acosta-Alonzo *et al.*[10] explored the vaccination landscape against typhoid fever in rural areas of Ghana and investigated whether low vaccination coverage could be attributed to rational behavior among individuals. Adapting a model from Mushayabasa,[13] they considered chronic lifelong carriers, short-cycle transmissions in the immediate environment, and long-cycle transmissions via water supply contamination. However, a limitation was identified in the Mushayabasa model, which failed to incorporate an exposed compartment crucial for understanding typhoid transmission dynamics due to the incubation period of the disease. Addressing this gap is essential for refining models that demonstrate the complexity of typhoid spread. These studies collectively provide valuable insights into the evolving landscape of mathematical epidemiology, emphasizing the need for an inclusive approach to effectively model and combat typhoid fever. In this study, we address a critical gap in the existing research by developing a comprehensive model that incorporates crucial factors and captures the essential features of typhoid transmission dynamics.

The subsequent sections of this paper are as follows: in Sec. II, we formulate the model and introduce the essential definitions for our investigation. In Sec. III, we investigate the model analysis covering the disease-free equilibrium point, basic reproduction number, and endemic equilibrium point. In Sec. IV, we demonstrate the fundamental definitions and concepts of fractional calculus and transform the model to a system of Caputo-fractional derivative. Section V presents numerical simulations, followed by a detailed discussion of our findings and conclusion in Sec. VI.

II. DESCRIPTION AND FORMULATION OF THE MODEL

It is assumed that everyone in the population has an equal probability of acquiring the infection and that the population is homogeneously mixed. We take into account both the transmission from person to person and the transmission through the environment as a result of contact with *Salmonella typhi* bacteria in food and water. At time t, the model divides the entire human population $[N(t)]$ into six (6) different compartments that do not overlap, including susceptible individuals $[S(t)]$, vaccinated individuals $[V(t)]$, exposed individuals $[E(t)]$, asymptomatic infected individuals $[I_a(t)]$, symptomatic infected individuals $[I_v(t)]$, and individuals who have recovered and developed immunity from the infection $[R(t)]$, so that

$$N(t) = S(t) + V(t) + E(t) + I_a(t) + I_s(t) + R(t). \tag{1}$$

The equations describing the typhoid fever transmission with $q \in (0, 1)$ are

$$\frac{dS}{dt} = \Lambda + \omega V - (\lambda + \epsilon + \mu)S, \tag{2}$$

$$\frac{dV}{dt} = \epsilon S - ((1-\phi)\lambda + \omega + \mu)V, \tag{3}$$

$$\frac{dE}{dt} = \lambda S + (1-\phi)\lambda V + \rho\lambda R - (\sigma + \mu)E, \tag{4}$$

$$\frac{dI_a}{dt} = (1-\tau)\sigma E - (\varpi + \alpha + \mu)I_a, \tag{5}$$

$$\frac{dI_s}{dt} = \tau\sigma E + \varpi I_a - (\alpha(1-\theta\eta) + \delta_1 + \mu)I_s, \tag{6}$$

$$\frac{dR}{dt} = \alpha I_a + \alpha(1-\theta\eta)I_s - (\rho\lambda + \mu)R, \tag{7}$$

$$\frac{dC}{dt} = \gamma_1 I_a + \gamma_2 I_s - \delta_2 C, \tag{8}$$

where

$$\lambda = \frac{(1-\kappa)\beta[I_a + \nu_1 I_s + \nu_2 C]}{N}, \tag{9}$$

with the following non-negative initial conditions:

$$S(0) \geq 0, \quad V(0) \geq 0, \quad E(0) \geq 0, \quad I_a(0) \geq 0,$$
$$I_s(0) \geq 0, \quad R(0) \geq 0, \quad C(0) \geq 0.$$

Equation (2) represents the susceptible population, where individuals enter at a fixed rate Λ. This can occur either through birth or immigration or when a vaccinated individual loses immunity[14] and needs to be revaccinated. Individuals in this group are susceptible to infection upon contact with asymptomatic infected individuals (I_a), symptomatic infected individuals (I_s), or contaminated food or water (C).

Equation (3) characterizes the vaccination compartment. The first term signifies individuals transitioning from a susceptible pool after vaccination. Despite vaccination, breakthrough infections may occur because of the imperfect nature of the vaccine.[9] However, the transmission rate of these breakthrough infections is reduced by $(1-\phi)$, where ϕ denotes the vaccine efficacy.

Equation (4) represents the exposed compartment. In our scenario, individuals in this group were assumed to be non-infectious during the range from 9.7 to 21.2 days of typhoid fever incubation period.[15] A fraction of this population progresses to symptomatic infection at rate $\tau\sigma$, whereas others become asymptomatic at rate $(1-\tau)\sigma$.

Equations (5) and (6) correspond to two infected classes: asymptomatic and symptomatic infections, respectively. Asymptomatic individuals recover at rate α_1, whereas symptomatic infected individuals face mortality at rate δ_1. Symptomatic individuals can recover from the disease at rate $\alpha(1-\theta\eta)$, where θ represents the rate of antibiotic resistance and η signifies accessibility to the healthcare system (NB. $0 < \theta\eta < 1$).

Equation (7) monitors the recovered individuals constituting the immune/partially immune individuals. The first two terms indicate individuals recovering from the disease who may develop immunity or remain partially immune. This group is also susceptible to reinfection at the rate of $\rho(0 \leq \rho < 1\ )$.

In Eqs. (2) and (7), individuals experience natural death at a rate of μ.

Equation (8) represents the contaminated environment influenced by the shedding of bacteria from either asymptomatic or symptomatic infected compartments. Proper sanitation practices are also considered to affect the reduction rate of *Salmonella typhi* bacteria in this environment.

The description of the variables and parameters is tabulated in Tables I and II, respectively.

TABLE I. Meaning of variables.

Variable	Meaning
S	Susceptible individuals
V	Vaccinated individuals
E	Exposed individuals
I_a	Asymptomatic infected individuals
I_s	Symptomatic infected individuals
R	Recovered individuals
C	*Salmonella typhi* bacteria in the environment

TABLE II. Parameters and their meaning.

Parameter	Meaning and units
Λ	Rate at which new members enter the susceptible group
ω	Rate of individuals transitioning from V to S
ϵ	Rate of vaccination of susceptible individuals
μ	Natural death rate
ϕ	Reduction in transmission due to vaccine efficacy
ρ	Reinfection rate for recovered individuals
σ	Rate of progression from exposed to infected
τ	Fraction progressing to I_a from exposed
β	Effective contact rate
κ	Rate of reduction in infectiveness (by practicing safe sanitation)
ν_1	Rate of infectiousness of I_s
ν_2	Rate of infectiousness of C
α	Recovery rate of infected individuals
δ_1	Mortality rate of symptomatic infected individuals
δ_2	Reduction rate of bacteria in contaminated environment
$\bar{\omega}$	Progression rate from I_a to I_s
γ_1	Shedding rate of bacteria by I_a
γ_2	Shedding rate of bacteria by I_s
θ	Rate of antibiotic resistance
η	Accessibility to healthcare system

III. MODEL ANALYSIS

This model analysis assumed that individuals who have recovered but later lose immunity can play a role in the occurrence and transmission of typhoid fever. Following this, we established the fundamental properties of model equations (2)–(8).

A. Invariant region

The positivity of the model equations (2)–(8) is crucial, as it reflects the biological context of population densities, wherein the lowest possible value is zero. This is paramount for establishing an upper bound for the model.

Consider

$$\mathbb{X} = \left\{(S, V, E, I_a, I_s, R) \in \mathbb{R}_+^6 : N(t) \leq \frac{\Lambda}{\mu}, C(t) \in \mathbb{R}_+ : C(t) \leq \frac{(\gamma_1+\gamma_2)\Lambda}{\mu\delta_2}\right\}. \tag{10}$$

We establish that the closed set $\mathbb{X}$ is the feasible region for model equations (2)–(8).

Lemma 1. For the typhoid fever model defined by model equations (2)–(8), with initial condition $s(0) > 0, V(0) > 0, E(0) \geq 0, I_a(0) \geq 0, I_s(0) \geq 0, R(0) \geq 0,$ *and* $C(0) \geq 0$, *the closed set* $\mathbb{X}$ *is positively invariant and biologically meaning ful for all* $t \geq 0$.

Proof. We begin by adding the entire human population as follows:

$$\frac{dN}{dt} = \Lambda - \mu N(t) - \delta_1 I_s(t) \leq \Lambda - \mu N(t),$$

$$\frac{dN}{dt} + \mu N \leq \Lambda,$$

$$N(t) \leq N(0)e^{-ut} + \frac{\Lambda}{\mu}(1 - e^{-ut}), \tag{11}$$

where $N(0)$ is the initial condition. As $t \to 0$ in (11), $N(t) \to \frac{\Lambda}{\mu}$. Thus, every solution to Eqs. (2)–(8) is applicable to the human population remaining within the defined region continuously.

To ensure the positivity of the state variables, we present and establish the following lemma. □

Lemma 2. Consider the model given by Eqs. (2)–(8) under the following initial conditions: $S(0) > 0, V(0) \geq 0, E(0) \geq 0, I_a(0) \geq 0, I_s(0) \geq 0, R(0) \geq 0,$ *and* $C(0) \geq 0$. *Then, the solutions* $\{S, V, E, I_a, I_s, R, C\}$ *are positive in* $\mathbb{R}^7_+$.

Proof. Utilizing an approach similar to that in Ref. 16, we initially focus on Eq. (2), given by

$$\frac{dS}{dt} = \Lambda + \omega V - (\lambda + \epsilon + \mu)S, \tag{12}$$

where $t_1 = \sup\{t > 0 : S > 0, V > 0, E > 0, I_a > 0, I_s > 0, R > 0, C > 0, \} \in [0, t]$. Since $t_1 > 0$, Eq. (12) implies that

$$\frac{dS}{dt} \geq \Lambda - (\lambda + \epsilon + \mu)S. \tag{13}$$

Equation (13) can be reformulated as

$$\frac{dS}{dt} + (\lambda + \epsilon + \mu)S \geq \Lambda, \tag{14}$$

resulting in

$$\frac{d}{dt}\left[S(t)\exp\left\{(\epsilon+\mu)t + \int_0^t \lambda(u)du\right\}\right] \geq \Lambda \exp\left\{(\epsilon+\mu)t + \int_0^t \lambda(u)du\right\}. \tag{15}$$

Consequently,

$$S(t_1)\exp\left\{(\epsilon+\mu)t_1 + \int_0^{t_1}\lambda(u)du\right\} - S(0) \geq \int_0^{t_1} \Lambda \exp\left\{(\epsilon+\mu)x + \int_0^x \lambda(v)dv\right\}dx, \tag{16}$$

leading to

$$\begin{aligned} S(t_1) &= S(0)\exp\left\{-(\epsilon+\mu)t_1 - \int_0^{t_1}\lambda(u)du\right\} \\ &\quad + \exp\left\{-(\epsilon+\mu)t_1 - \int_0^{t_1}\lambda(u)du\right\} \\ &\quad \times\left[\int_0^{t_1}\Lambda\exp\left\{(\epsilon+\mu)x + \int_0^x\lambda(v)dv\right\}dx\right] > 0. \end{aligned} \tag{17}$$

By employing a similar approach, it can be demonstrated that $V(t), E(t), I_a(t), I_s(t), R(t),$ and $C(t)$ are always positive for $t > 0$. This implies that all solutions of Eqs. (2)–(8) remain positive under all non-negative initial conditions, as anticipated. □

As a result, we can affirm that within domain $\mathbb{X}$, the proposed model is well posed and holds significance from both epidemiological and mathematical perspectives.

B. Disease-free equilibrium

The equilibrium state without the presence of the disease, referred to as disease-free equilibrium (DFE), in model equations (2)–(8) is expressed as

$$\begin{aligned} \text{DFE} &= \{S^*, V^*, E^*, I_a^*, I_s^*, R^*, C^*\} \\ &= \left\{\frac{(\mu+\omega)\Lambda}{\mu(\epsilon+\mu+\omega)}, \frac{\epsilon\Lambda}{\mu(\epsilon+\mu+\omega)}, 0, 0, 0, 0, 0\right\}. \end{aligned}$$

1. Basic reproduction number

In this case, we calculated the basic reproduction number (R_0) for the typhoid fever model equations (2)–(8) using the next-generation matrix (NGM) technique, as illustrated in Ref. 17. R_0 signifies the number of secondary cases that a typical primary case would generate throughout the infectious period in an entirely susceptible population.[18–20] Matrices $\mathcal{F}$, representing the new infection terms, and $\mathcal{V}$, denoting the other transfer terms, are as follows:

$$\mathcal{F} = \begin{bmatrix} \lambda S + c_2\lambda V + \rho\lambda R \\ 0 \\ 0 \\ 0 \end{bmatrix}, \quad \mathcal{V} = \begin{bmatrix} n_1 E \\ -c_3\sigma E + n_2 I_a \\ -\tau\sigma E - \varpi I_a + n_3 I_s \\ -\gamma_1 I_a - \gamma_2 I_s + \delta_2 C \end{bmatrix}, \tag{18}$$

where

$$c_1 = 1 - \kappa, \quad c_2 = 1 - \phi, \quad c_3 = 1 - \tau, \quad c_4 = 1 - \theta\eta,$$
$$n_1 = \sigma + \mu, \quad n_2 = \varpi + \alpha + \mu,$$
$$n_3 = \alpha c_4 + \delta_1 + \mu, \quad n_4 = \epsilon + \mu + \omega, \quad \text{and} \quad n_5 = c_1(c_2\epsilon + \mu + \omega).$$

$$F = \begin{bmatrix} 0 & \frac{\beta n_5}{n_4} & \frac{v_1\beta n_5}{n_4} & \frac{v_2\beta n_5}{n_4} \\ 0 & 0 & 0 & 0 \\ 0 & 0 & 0 & 0 \\ 0 & 0 & 0 & 0 \end{bmatrix}, \quad V = \begin{bmatrix} n_1 & 0 & 0 & 0 \\ -c_3\sigma & n_2 & 0 & 0 \\ -\tau\sigma & -\varpi & n_3 & 0 \\ 0 & -\gamma_1 & -\gamma_2 & \delta_2 \end{bmatrix}. \tag{19}$$

Therefore,

$$R_0 = \frac{\sigma\beta[c_3 n_3\delta_2 + (\tau\delta_2 n_2 + \omega c_3\delta_2)\nu_1 + (\tau\gamma_2 n_2 + \omega c_3\gamma_2 + c_3\gamma_1 n_3)\nu_2]n_5}{n_1 n_2 n_3 n_4 \delta_2}. \tag{20}$$

Hence, we have the following lemma.

Lemma 3. The DFE of Eqs. (2)–(8) is locally asymptotically stable (LAS) if and only if the value of $R_0 < 1$. Conversely, if $R_0 > 1$, then the DFE is unstable.

C. Global stability of the disease-free equilibrium (DFE)

We investigated the global stability of the disease-free equilibrium (DFE) utilizing the method by Castillo-Chavez *et al.*[21] Consider the following equations:

$$\begin{aligned} \frac{dX}{dt} &= F(X, Y), \\ \frac{dY}{dt} &= G(X, Y), \quad \text{with} \quad G(X, 0) = 0. \end{aligned} \tag{21}$$

$X \in \mathbb{R}^m$ denotes non-infected compartments, $Y \in \mathbb{R}^n$ denotes infected compartments, and DFE represents the disease-free equilibrium of the system. Castillo-Chavez *et al.* established that the global asymptotic stability of the DFE is achieved when the following two specified conditions are met:

(B1) $\frac{dX}{dt} = F(X, 0)$, and X^* is globally asymptotically stable.
(B2) $G(X, Y) = BY - \hat{G}(X, Y)$, where $\hat{G}(X, Y) \geq 0$ for all (X, Y) in the biologically meaningful domain $\mathbb{X}$ and $B = D_Y G(X^*, 0)$ is an M-matrix.

Therefore, the following theorem is proposed.

Theorem 4 *(Castillo-Chavez et al.[21]). If $R_0 < 1$ (LAS), and assumptions (B1) and (B2) hold, then DFE is globally asymptotically stable for the system.*

This result can be applied to our model equations (2)–(8) to conclude the following.

Theorem 5. *The DFE of model equation (8) is globally asymptotically stable if $R_0 < 1$.*

Proof. We start by decomposing Eqs. (2)–(8) into subsystems of susceptible humans, vaccinated humans, and recovered humans, denoted by

$$X = (S, V, R), \tag{22}$$

and exposed humans, infected humans, and the concentration of *Salmonella typhi* in the salmonella-contaminated environment, denoted by

$$Y = (E, I_a, I_s, C). \tag{23}$$

To ensure global stability, we rewrite the model equations (2)–(8) as shown in Eq. (21), where $X \in \mathbb{R}^3$ and $Y \in \mathbb{R}^3$. With this new formulation, the DFE is now denoted as DFE $= (X_0, \mathbf{0})$, where $X_0 = \left(\frac{(\mu+\omega)\Lambda}{\mu n_4}, \frac{\epsilon\Lambda}{\mu n_4}, 0\right)$ is an equilibrium point of the reduced system,

$$\frac{dX}{dt} = F(X, \mathbf{0}). \tag{24}$$

To attain the global stability of the disease-free equilibrium, it is imperative to fulfill the following specified conditions, referred to as (B1) and (B2):

(B1) X_0 is a globally asymptotically stable equilibrium for $\frac{dX}{dt} = F(X_0, \mathbf{0})$.
(B2) $G(X, Y) = BY - \hat{G}(X, Y)$, where $\hat{G}(X, Y) \geq 0$ for all $(X, Y) \in \mathbb{X}$.

The matrices B and $\hat{G}(X, Y)$ are defined as follows:

$$B = D_Y G(X^*, 0) = \begin{bmatrix} -n_1 & \frac{\beta n_5}{n_4} & \frac{\nu_1\beta n_5}{n_4} & \frac{\nu_2\beta n_5}{n_4} \\ c_3\sigma & -n_2 & 0 & 0 \\ \tau\sigma & \omega & -n_3 & 0 \\ 0 & \gamma_1 & \gamma_2 & -\delta_2 \end{bmatrix} \tag{25}$$

and

$$\hat{G}(X, Y) = \begin{bmatrix} (I_a + \nu_1 I_s + \nu_2 C)\left[1 - \frac{c_1[S + c_2 V + \rho R]}{N} \cdot \frac{n_4}{n_5}\right] \\ 0 \\ 0 \\ 0 \end{bmatrix}. \tag{26}$$

Since $n_4 < n_5$, $\hat{G}(X, Y) \geq 0$. Hence, (B2) is satisfied and the DFE is globally asymptotically stable. □

D. Existence of endemic equilibrium point (EE)

The equilibrium states (denoted as EE) of the model [Eqs. (2)–(8)] represent the endemic equilibrium where the disease has the potential to persist within the population. These equilibria occur when at least one of the infected classes is nonempty, indicating the presence of sustained infection dynamics. This insight is crucial for understanding the long-term behavior of the mathematical epidemiological model.

Let $EE = (S^{**}, V^{**}, E^{**}, I_a^{**}, I_s^{**}, R^{**}, C^{**})$ be the EE for the model [Eqs. (2)–(8)], which in terms of the force of infection λ^{**} is given by

$$\begin{aligned} S^{**} &= \frac{\Lambda(n_7 + c_2\lambda^{**})}{c_2\lambda^{**^2} + (n_7 + c_2 n_6)\lambda^{**} + \mu^2 + (\epsilon + \omega)\mu}, \\ V^{**} &= \frac{\Lambda\epsilon}{c_2\lambda^{**^2} + (n_7 + c_2 n_6)\lambda^{**} + \mu^2 + (\epsilon + \omega)\mu}, \\ I_a^{**} &= \frac{c_3\sigma E^{**}}{n_2}, \\ I_s^{**} &= \frac{\sigma(\tau n_2 + c_3\varpi)E^*}{n_2 n_3}, \\ R^{**} &= \frac{\sigma\alpha(c_3 n_3 + c_4(\tau n_2 + c_3\varpi))E^{**}}{(\lambda^{**}\rho + \mu)n_2 n_3}, \\ C^{**} &= \frac{\sigma(\tau\gamma_2 n_2 + c_3\varpi\gamma_2 + c_3\gamma_1 n_3)E^{**}}{n_2 n_3\delta_2}, \end{aligned} \tag{27}$$

where $n_6 = \epsilon + \mu, n_7 = \omega + \mu$,

$$\lambda = \frac{c_1\beta\left[I_a^{**} + \nu_1 I_s^{**} + \nu_2 C^{**}\right]}{N^{**}}, \tag{28}$$

and

$$N^{**} = S^{**} + V^{**} + E^{**} + I_a^{**} + I_s^{**} + R^{**}. \tag{29}$$

Equation (31) can now be written as

$$\begin{aligned} &S^{**} + V^{**} + E^{**} + \left(1 - \frac{c_1\beta}{\lambda^{**}}\right)I_a^{**} \\ &+ \left(1 - \frac{c_1\beta\nu_1}{\lambda^{**}}\right)I_s^{**} - \frac{c_1\beta\nu_2}{\lambda^{**}}C + R = 0, \end{aligned} \tag{30}$$

so the nonzero (endemic) equilibria of model equations (2)–(8) satisfy the following criteria:

$$a_1(\lambda^{**})^3 + a_2(\lambda^{**})^2 + a_3\lambda^{**} + a_4 = 0, \tag{31}$$

where

$$\begin{aligned} a_1 &= \delta_2\rho c_2(((n_3 + \varpi)c_3 + n_2\tau)\sigma + n_2 n_3), \\ a_2 &= -\beta\rho\sigma\tau c_1 c_2\delta_2 n_2\nu_1 - \beta\rho\sigma\tau c_1 c_2\gamma_2 n_2\nu_2 - \beta\rho\sigma\varpi c_1 c_2 c_3\delta_2\nu_1 - \beta\rho\sigma\varpi c_1 c_2 c_3\gamma_2\nu_2 \\ &\quad - \beta\rho\sigma c_1 c_2 c_3\gamma_1 n_3\nu_2 - \alpha\rho\sigma\tau c_2 c_4\delta_2 n_2 - \alpha\rho\sigma\varpi c_2 c_3 c_4\delta_2 - \beta\rho\sigma c_1 c_2 c_3\delta_2 n_3 - \alpha\rho\sigma c_2 c_3\delta_2 n_3 \\ &\quad + \alpha\sigma\tau c_2 c_4\delta_2 n_2 + \alpha\sigma\varpi c_2 c_3 c_4\delta_2 + \epsilon\rho\sigma\tau c_2\delta_2 n_2 + \epsilon\rho\sigma\varpi c_2 c_3\delta_2 + \epsilon\rho\sigma c_2 c_3\delta_2 n_3 + \alpha\sigma c_2 c_3\delta_2 n_3 \\ &\quad + \epsilon\rho c_2\delta_2 n_2 n_3 + \mu\sigma\tau c_2\delta_2 n_2 + \mu\sigma\varpi c_2 c_3\delta_2 + \mu\sigma c_2 c_3\delta_2 n_3 + \rho\sigma\tau\delta_2 n_2 n_7 + \rho\sigma\varpi c_3\delta_2 n_7 + \rho\sigma c_3\delta_2 n_3 n_7 \\ &\quad + \rho c_2\delta_2 n_1 n_2 n_3 + \mu c_2\delta_2 n_2 n_3 + \rho\delta_2 n_2 n_3 n_7, \\ a_3 &= -\beta\epsilon\rho\sigma\tau c_1 c_2\delta_2 n_2\nu_1 - \beta\epsilon\rho\sigma\tau c_1 c_2\gamma_2 n_2\nu_2 - \beta\epsilon\rho\sigma\varpi c_1 c_2 c_3\delta_2\nu_1 - \beta\epsilon\rho\sigma\varpi c_1 c_2 c_3\gamma_2\nu_2 \\ &\quad - \beta\epsilon\rho\sigma c_1 c_2 c_3\gamma_1 n_3\nu_2 - \beta\epsilon\rho\sigma c_1 c_2 c_3\delta_2 n_3 - \beta\mu\sigma\tau c_1 c_2\delta_2 n_2\nu_1 - \beta\mu\sigma\tau c_1 c_2\gamma_2 n_2\nu_2 - \beta\mu\sigma\varpi c_1 c_2 c_3\delta_2\nu_1 \\ &\quad - \beta\mu\sigma\varpi c_1 c_2 c_3\gamma_2\nu_2 - \beta\mu\sigma c_1 c_2 c_3\gamma_1 n_3\nu_2 - \beta\rho\sigma\tau c_1\delta_2 n_2 n_7\nu_1 - \beta\rho\sigma\tau c_1\gamma_2 n_2 n_7\nu_2 - \beta\rho\sigma\varpi c_1 c_3\delta_2 n_7\nu_1 \\ &\quad - \beta\rho\sigma\varpi c_1 c_3\gamma_2 n_7\nu_2 - \beta\rho\sigma c_1 c_3\gamma_1 n_3 n_7\nu_2 - \alpha\epsilon\rho\sigma\tau c_4\delta_2 n_2 - \alpha\epsilon\rho\sigma\varpi c_3 c_4\delta_2 + \alpha\epsilon\sigma\tau c_2 c_4\delta_2 n_2 \\ &\quad + \alpha\epsilon\sigma\varpi c_2 c_3 c_4\delta_2 - \alpha\rho\sigma\tau c_4\delta_2 n_2 n_7 - \alpha\rho\sigma\varpi c_3 c_4\delta_2 n_7 - \beta\mu\sigma c_1 c_2 c_3\delta_2 n_3 - \beta\rho\sigma c_1 c_3\delta_2 n_3 n_7 \\ &\quad - \alpha\epsilon\rho\sigma c_3\delta_2 n_3 + \alpha\epsilon\sigma c_2 c_3\delta_2 n_3 - \alpha\rho\sigma c_3\delta_2 n_3 n_7 + \alpha\sigma\tau c_4\delta_2 n_2 n_7 + \alpha\sigma\varpi c_3 c_4\delta_2 n_7 + \epsilon\mu\sigma\tau c_2\delta_2 n_2 \\ &\quad + \epsilon\mu\sigma\varpi c_2 c_3\delta_2 + \epsilon\mu\sigma c_2 c_3\delta_2 n_3 + \alpha\sigma c_3\delta_2 n_3 n_7 + \epsilon\mu c_2\delta_2 n_2 n_3 + \epsilon\rho\delta_2 n_1 n_2 n_3 + \mu\sigma\tau\delta_2 n_2 n_7 \\ &\quad + \mu\sigma\varpi c_3\delta_2 n_7 + \mu\sigma c_3\delta_2 n_3 n_7 + \mu c_2\delta_2 n_1 n_2 n_3 + \rho\delta_2 n_1 n_2 n_3 n_7 + \mu\delta_2 n_2 n_3 n_7, \\ a_4 &= \mu n_3 n_2 n_4 n_1\delta_2(1 - R_0). \end{aligned} \tag{32}$$

From Eq. (35), it is evident that a_1 is positive because of the non-negativity of all model parameters. In addition, for $R_0 < 1$, a_4 is positive, whereas for $R_0 > 1$, it is negative. Consequently, the potential real roots of polynomial (34) are influenced by the signs of a_2, a_3, and a_4. Descartes' rule of signs can be utilized to analyze this cubic function, leading to the following conclusions. Table III summarizes the various scenarios for the roots of Eq. (34).[22,23]

IV. THE TYPHOID FEVER FRACTIONAL MODEL

Models based on fractional-order calculus are highly effective for simulating disease transmission dynamics. These models capture disease spread more thoroughly and accurately than traditional integer-order models. By integrating fractional order into the modeling of typhoid epidemics, we gained a deeper and more

TABLE III. Number of possible positive real roots of (34).

Case	a_1	a_2	a_3	a_4	R_0	No. of sign changes	No. of +ve real roots
i	+	+	+	+	$R_0 < 1$	0	0
ii	+	+	+	−	$R_0 > 1$	1	1
iii	+	+	−	+	$R_0 < 1$	2	0, 2
iv	+	+	−	−	$R_0 > 1$	1	1
v	+	−	+	+	$R_0 < 1$	2	0, 2
vi	+	−	+	−	$R_0 > 1$	3	1, 3
vii	+	−	−	+	$R_0 < 1$	2	0, 2
viii	+	−	−	−	$R_0 > 1$	1	1

precise understanding of how the disease spreads. This enhanced understanding is crucial for making well-informed decisions and effectively reducing the impact of an endemic. In our study, we opted for the Caputo fractional operator because of its compatibility with the initial and boundary conditions, along with its consistent behavior with constants, aligning with the principles of classical calculus.

A. Preliminary definitions and model formulation

We begin with the following definitions.

Definition 6. Let $g(t)$ be an integrable function, and the Caputo derivative of fractional order $q \in (0,1)$ is given by

$$ {}^{C}\mathbb{D}_t^q g(t) = \frac{1}{\Gamma(m-q)} \int_0^t \frac{g^{(m)}(\varphi)}{(t-\varphi)^{q-m+1}} d\varphi, \tag{33} $$

where

$$ m \in \mathbb{N} \quad \text{and} \quad m \in (m-1, m), $$

and

$$ {}^{C}\mathbb{D}_t^q g(t) = \frac{1}{\Gamma(1-q)} \int_0^t (t-\varphi)^{-q} g'(\varphi) d\varphi, \tag{34} $$

for $m = 1$ and $q \in (0,1]$. In addition, the corresponding fractional integral of order $q > 0$ is defined as

$$ {}^{C}\mathbb{I}_t^q g(t) = \frac{1}{\Gamma(q)} \int_0^t (t-\varphi)^{q-1} g(\varphi) d\varphi. \tag{35} $$

See Refs. 24 and 25.

The equations describing the fractional-order typhoid fever transmission model with $q \in (0,1)$ are formulated as follows:

$$ \begin{aligned}
\chi^{q-1}\, {}^{C}\mathbb{D}_t^q[S(t)] &= \Lambda + \omega V - (\lambda + \epsilon + \mu)S, \\
\chi^{q-1}\, {}^{C}\mathbb{D}_t^q[V(t)] &= \epsilon S - ((1-\phi)\lambda + \omega + \mu)V, \\
\chi^{q-1}\, {}^{C}\mathbb{D}_t^q[E(t)] &= \lambda S + (1-\phi)\lambda V + \rho\lambda R - (\sigma + \mu)E, \\
\chi^{q-1}\, {}^{C}\mathbb{D}_t^q[I_a(t)] &= (1-\tau)\sigma E - (\varpi + \alpha + \mu)I_a, \\
\chi^{q-1}\, {}^{C}\mathbb{D}_t^q[I_s(t)] &= \tau\sigma E + \varpi I_a - (\alpha(1-\theta\eta) + \delta_1 + \mu)I_s, \\
\chi^{q-1}\, {}^{C}\mathbb{D}_t^q[R(t)] &= \alpha I_a + \alpha(1-\theta\eta)I_s - (\rho\lambda + \mu)R, \\
\chi^{q-1}\, {}^{C}\mathbb{D}_t^q[C(t)] &= \gamma_1 I_a + \gamma_2 I_s - \delta_2 C,
\end{aligned} \tag{36} $$

with the following initial conditions:

$$ \begin{aligned}
S(0) = S_0, \quad V(0) = V_0, \quad E(0) = E_0, \quad I_a(0) = I_{a_0}, \\
I_s(0) = I_{s_0}, \quad R(0) = R_0, \quad C(0) = C_0,
\end{aligned} $$

where

$$ \lambda = \frac{(1-\kappa)\beta[I_a + \nu_1 I_s + \nu_2 C]}{N}, \tag{37} $$

${}^{C}\mathbb{D}_t^q(\cdot)$ represents the Caputo-fractional operator, and χ is the auxiliary parameter (see Refs. 24 and 26) that resolves the dimension issue.

B. Existence and uniqueness of solutions of (36)

This subsection demonstrates the existence of a unique solution to the fractional model, which is given by Eq. (36). Taking the Caputo fractional-integral on both sides of (36), we have the following:

$$ \begin{aligned}
S(t) - S(0) &= {}^{C}\mathbb{I}_t^q\{\Lambda + \omega V - (\lambda + \epsilon + \mu)S\}, \\
V(t) - V(0) &= {}^{C}\mathbb{I}_t^q\{\epsilon S - ((1-\phi)\lambda + \omega + \mu)V\}, \\
E(t) - E(0) &= {}^{C}\mathbb{I}_t^q\{\lambda S + (1-\phi)\lambda V + \rho\lambda R - (\sigma + \mu)E\}, \\
I_a(t) - I_a(0) &= {}^{C}\mathbb{I}_t^q\{(1-\tau)\sigma E - (\varpi + \alpha + \mu)I_a\}, \\
I_s(t) - I_s(0) &= {}^{C}\mathbb{I}_t^q\{\tau\sigma E + \varpi I_a - (\alpha(1-\theta\eta) + \delta_1 + \mu)I_s\}, \\
R(t) - R(0) &= {}^{C}\mathbb{I}_t^q\{\alpha I_a + \alpha(1-\theta\eta)I_s - (\rho\lambda + \mu)R\}, \\
C(t) - C(0) &= {}^{C}\mathbb{I}_t^q\{\gamma_1 I_a + \gamma_2 I_s - \delta_2 C\}.
\end{aligned} \tag{38} $$

Applying the integral, (35) and (38) can now become

$$ \begin{aligned}
S(t) &= S(0) + \frac{\chi^{1-q}}{\Gamma(q)} \int_0^t G_1(\varphi, S)(t-\varphi)^{q-1} d\varphi, \\
V(t) &= V(0) + \frac{\chi^{1-q}}{\Gamma(q)} \int_0^t G_2(\varphi, V)(t-\varphi)^{q-1} d\varphi, \\
E(t) &= E(0) + \frac{\chi^{1-q}}{\Gamma(q)} \int_0^t G_3(\varphi, E)(t-\varphi)^{q-1} d\varphi, \\
I_a(t) &= I_a(0) + \frac{\chi^{1-q}}{\Gamma(q)} \int_0^t G_4(\varphi, I_a)(t-\varphi)^{q-1} d\varphi, \\
I_s(t) &= I_s(0) + \frac{\chi^{1-q}}{\Gamma(q)} \int_0^t G_5(\varphi, I_s)(t-\varphi)^{q-1} d\varphi, \\
R(t) &= R(0) + \frac{\chi^{1-q}}{\Gamma(q)} \int_0^t G_6(\varphi, R)(t-\varphi)^{q-1} d\varphi, \\
C(t) &= C(0) + \frac{\chi^{1-q}}{\Gamma(q)} \int_0^t G_7(\varphi, C)(t-\varphi)^{q-1} d\varphi.
\end{aligned} \tag{39} $$

The nonlinear functions on the right-hand side of Eq. (36) are defined as G_i, where i ranges from 1 to 7. We demonstrate that these functions satisfy both the Lipschitz condition and contraction.

Theorem 7. *The kernels G_1 satisfy the Lipschitz condition and contraction if*

$$0 \leq (n_6 + l) < 1. \tag{40}$$

Proof. For S and S_1, we have the following:

$$\begin{aligned}\|G_1(t,S) - G_1(t,S_1)\| &= \|-(n_6+\lambda)S(t) + (n_6+\lambda)S_1(t)\| \\ &\leq \|(n_6)+\lambda\|\|S(t) - S_1(t)\| \\ &\leq (n_6 + \|\lambda\|)\|S(t) - S_1(t)\|.\end{aligned}$$

If we let $k_1 = (n_6 + l)$, where $\|\lambda\| \leq l$ is a bounded function,

$$\|G_1(t,S) - G_1(t,S_1)\| \leq k_1\|S(t) - S_1(t)\|. \tag{41}$$

Therefore, in the case of G_1, the Lipschitz condition is fulfilled, and it becomes a contraction if $0 \leq (n_6 + l) < 1$. □

Similarly, the Lipschitz condition for $G_i's : i = 2, 3, 4, 5, 6,$ and 7 is as follows:

$$\begin{aligned}\|G_2(t,V(t)) - G_2(t,V_1(t))\| &\leq k_2\|V(t) - V_1(t)\|, \\ \|G_3(t,E(t)) - G_3(t,E_1(t))\| &\leq k_3\|E(t) - E_1(t)\|, \\ \|G_4(t,I_a(t)) - G_4(t,I_{a_1}(t))\| &\leq k_4\|I_a(t) - I_{a_1}(t)\|, \\ \|G_5(t,I_s(t)) - G_5(t,I_{s_1}(t))\| &\leq k_5\|I_s(t) - I_{s_1}(t)\|, \\ \|G_6(t,R(t)) - G_6(t,R_1(t))\| &\leq k_6\|R(t) - R_1(t)\|, \\ \|G_7(t,C(t)) - G_7(t,C_1(t))\| &\leq k_7\|C(t) - C_1(t)\|.\end{aligned} \tag{42}$$

In cases where $k_2 = (n_7 + c_2 l), k_3 = n_1, k_4 = n_2, k_5 = n_3, k_6 = (\mu + \rho l)$, and $k_7 = \delta_2$ are bounded functions, with $0 \leq k_i < 1$ for $i = 2, 3, 4, 5, 6, 7$, it follows that G_i for $i = 2, 3, 4, 5, 6, 7$ are contraction.

Recursive formulations derived from Eq. (39), labeled H_{in} for $i = 1, 2, \ldots, 7$, are used in establishing the uniqueness of the problem. These formulations yield the following set of equations:

$$\begin{aligned}H_{1n}(t) &= S_n(t) - S_{n-1}(t) = \frac{\chi^{1-q}}{\Gamma(q)}\int_0^t (G_1(\varphi, S_{n-1}(\varphi)) - G_1(\varphi, S_{n-2}(\varphi)))(t-\varphi)^{q-1}d\varphi, \\ H_{2n}(t) &= V_n(t) - V_{n-1}(t) = \frac{\chi^{1-q}}{\Gamma(q)}\int_0^t (G_2(\varphi, V_{n-1}(\varphi)) - G_2(\varphi, V_{n-2}(\varphi)))(t-\varphi)^{q-1}d\varphi, \\ H_{3n}(t) &= E_n(t) - E_{n-1}(t) = \frac{\chi^{1-q}}{\Gamma(q)}\int_0^t (G_3(\varphi, E_{n-1}(\varphi)) - G_3(\varphi, E_{n-2}(\varphi)))(t-\varphi)^{q-1}d\varphi, \\ H_{4n}(t) &= I_{a_n}(t) - I_{a_{n-1}}(t) = \frac{\chi^{1-q}}{\Gamma(q)}\int_0^t (G_4(\varphi, I_{a_{n-1}}(\varphi)) - G_4(\varphi, I_{a_{n-2}}(\varphi)))(t-\varphi)^{q-1}d\varphi, \\ H_{5n}(t) &= I_{s_n}(t) - I_{s_{n-1}}(t) = \frac{\chi^{1-q}}{\Gamma(q)}\int_0^t (G_5(\varphi, I_{s_{n-1}}(\varphi)) - G_5(\varphi, I_{s_{n-2}}(\varphi)))(t-\varphi)^{q-1}d\varphi, \\ H_{6n}(t) &= R_n(t) - R_{n-1}(t) = \frac{\chi^{1-q}}{\Gamma(q)}\int_0^t (G_6(\varphi, R_{n-1}(\varphi)) - G_6(\varphi, R_{n-2}(\varphi)))(t-\varphi)^{q-1}d\varphi, \\ H_{7n}(t) &= C_n(t) - C_{n-1}(t) = \frac{\chi^{1-q}}{\Gamma(q)}\int_0^t (G_7(\varphi, C_{n-1}(\varphi)) - G_7(\varphi, C_{n-2}(\varphi)))(t-\varphi)^{q-1}d\varphi,\end{aligned} \tag{43}$$

with initial conditions $S_0(t) = S(0), V_0(t) = V(0), E_0(t) = E(0), I_{a_0}(t) = I_a(0)$, $I_{s_0}(t) = I_s(0), R_0(t) = R(0),$ and $C_0(t) = C(0)$.

Applying the norm to the first equation in Eq. (43), we have the following:

$$\begin{aligned}\|H_{1n}(t)\| &= \|S_n(t) - S_{n-1}(t)\| \\ &= \left\|\frac{\chi^{1-q}}{\Gamma(q)}\int_0^t (G_1(\varphi, S_{n-1}(\varphi)) - G_1(\varphi, S_{n-2}(\varphi)))(t-\varphi)^{q-1}d\varphi\right\| \\ &\leq \frac{\chi^{1-q}}{\Gamma(q)}\int_0^t (t-\varphi)^{q-1}\|(G_1(\varphi, S_{n-1}(\varphi)) - G_1(\varphi, S_{n-2}(\varphi)))\|d\varphi.\end{aligned} \tag{44}$$

With (41), the following holds:

$$\|H_{1n}(t)\| \leq \frac{\chi^{1-q}}{\Gamma(q)}k_1\int_0^t (t-\varphi)^{q-1}\|H_{1(n-1)}(\varphi)\|d\varphi. \tag{45}$$

Similarly, we have

$$\begin{aligned}
\|H_{2n}(t)\| &\le \frac{\chi^{1-q}}{\Gamma(q)}k_2\int_0^t (t-\varphi)^{q-1}\|H_{2(n-1)}(\varphi)\|d\varphi,\\
\|H_{3n}(t)\| &\le \frac{\chi^{1-q}}{\Gamma(q)}k_3\int_0^t (t-\varphi)^{q-1}\|H_{3(n-1)}(\varphi)\|d\varphi,\\
\|H_{4n}(t)\| &\le \frac{\chi^{1-q}}{\Gamma(q)}k_4\int_0^t (t-\varphi)^{q-1}\|H_{4(n-1)}(\varphi)\|d\varphi,\\
\|H_{5n}(t)\| &\le \frac{\chi^{1-q}}{\Gamma(q)}k_5\int_0^t (t-\varphi)^{q-1}\|H_{5(n-1)}(\varphi)\|d\varphi,\\
\|H_{6n}(t)\| &\le \frac{\chi^{1-q}}{\Gamma(q)}k_6\int_0^t (t-\varphi)^{q-1}\|H_{6(n-1)}(\varphi)\|d\varphi,\\
\|H_{7n}(t)\| &\le \frac{\chi^{1-q}}{\Gamma(q)}k_7\int_0^t (t-\varphi)^{q-1}\|H_{7(n-1)}(\varphi)\|d\varphi.
\end{aligned} \tag{46}$$

Thus, we can write that

$$S_n(t)=\sum_{i=0}^{n}H_{1i}(t),\quad V_n(t)=\sum_{i=0}^{n}H_{2i}(t),\quad E_n(t)=\sum_{i=0}^{n}H_{3i}(t),$$
$$I_{a_n}(t)=\sum_{i=0}^{n}H_{4i}(t),$$

$$I_{s_n}(t)=\sum_{i=0}^{n}H_{5i}(t),\quad R_n(t)=\sum_{i=0}^{n}H_{6i}(t),\quad C_n(t)=\sum_{i=0}^{n}H_{7i}(t).$$

Hence, we establish the existence of a solution.

Theorem 8. *The fractional-order model given by Eq. (36) exhibits a set of solutions, provided that there is a time point t_1 such that the inequality $\frac{\chi^{1-q}}{\Gamma(q)}k_i t_1 < 1$, $i = 1, 2, \ldots, 7$, holds.*

Proof. By utilizing the recursive method described in Eqs. (45) and (46), we obtain

$$\begin{aligned}
\|H_{1n}(t)\| &\le \|S_n(0)\|\left[\frac{\chi^{1-q}}{\Gamma(q)}k_1 t\right]^n,\\
\|H_{2n}(t)\| &\le \|V_n(0)\|\left[\frac{\chi^{1-q}}{\Gamma(q)}k_2 t\right]^n,\\
\|H_{3n}(t)\| &\le \|E_n(0)\|\left[\frac{\chi^{1-q}}{\Gamma(q)}k_3 t\right]^n,\\
\|H_{4n}(t)\| &\le \|I_{a_n}(0)\|\left[\frac{\chi^{1-q}}{\Gamma(q)}k_4 t\right]^n,\\
\|H_{5n}(t)\| &\le \|I_{s_n}(0)\|\left[\frac{\chi^{1-q}}{\Gamma(q)}k_5 t\right]^n,\\
\|H_{6n}(t)\| &\le \|R_n(0)\|\left[\frac{\chi^{1-q}}{\Gamma(q)}k_6 t\right]^n,\\
\|H_{7n}(t)\| &\le \|C_n(0)\|\left[\frac{\chi^{1-q}}{\Gamma(q)}k_7 t\right]^n.
\end{aligned} \tag{47}$$

Therefore, there is a solution for the system that demonstrates continuity. By applying the subsequent assumption, we can demonstrate that Eq. (48) serves as the solution to Eq. (36),

$$\begin{aligned}
S(t)-S(0) &= S_n(t)-D_{1_n}(t),\\
V(t)-V(0) &= V_n(t)-D_{2_n}(t),\\
E(t)-E(0) &= E_n(t)-D_{3_n}(t),\\
I_a(t)-I_a(0) &= I_{a_n}(t)-D_{4_n}(t),\\
I_s(t)-I_s(0) &= I_{s_n}(t)-D_{5_n}(t),\\
R(t)-R(0) &= R_n(t)-D_{6_n}(t),\\
C(t)-C(0) &= C_n(t)-D_{7_n}(t).
\end{aligned} \tag{48}$$

$D_{1_n}(t), D_{2_n}(t), \ldots, D_{7_n}(t)$ represent the residual expressions of the solution. Therefore,

$$\begin{aligned}
\|D_{1_n}(t)\| &= \left\|\frac{\chi^{1-q}}{\Gamma(q)}\int_0^t (G_1(\varphi,S)-G_1(\varphi,S_{n-1}))d\varphi\right\|\\
&\le \frac{\chi^{1-q}}{\Gamma(q)}\int_0^t \|(G_1(\varphi,S)-G_1(\varphi,S_{n-1}))\|d\varphi\\
&\le \frac{\chi^{1-q}}{\Gamma(q)}k_1\|S-S_{n-1}\|t.
\end{aligned} \tag{49}$$

By repeating the method, we obtain

$$\|D_{1_n}(t)\| \le \left[\frac{\chi^{1-q}}{\Gamma(q)}t\right]^{n+1}k_1^{n+1}h. \tag{50}$$

TABLE IV. Summary of parameters with values, units, and references.

Parameter	Value	Unit	References
Λ	467	Person · day^{-1}	9 and 27
ω	9.041×10^{-4}	day^{-1}	9 and 13
ϵ	0.5000	–	9
μ	3.4562×10^{-4}	day^{-1}	Assumed
ϕ	0.4378	–	Assumed
ρ	0.5095	–	Assumed
σ	0.5000	day^{-1}	Assumed
τ	0.0931	day^{-1}	Assumed
β	0.8883	day^{-1}	Assumed
κ	0.2000	–	Assumed
ν_1	0.0019	day^{-1}	Assumed
ν_2	0.0790	day^{-1}	Assumed
α	0.8510	day^{-1}	11
$\delta 1$	0.0022	day^{-1}	11
$\delta 2$	0.0645	day^{-1}	11 and 27
ϖ	0.0020	day^{-1}	Assumed
γ_1	1	–	10
γ_2	1	–	9 and 27
θ	0.0070	–	Assumed
η	0.0030	–	Assumed

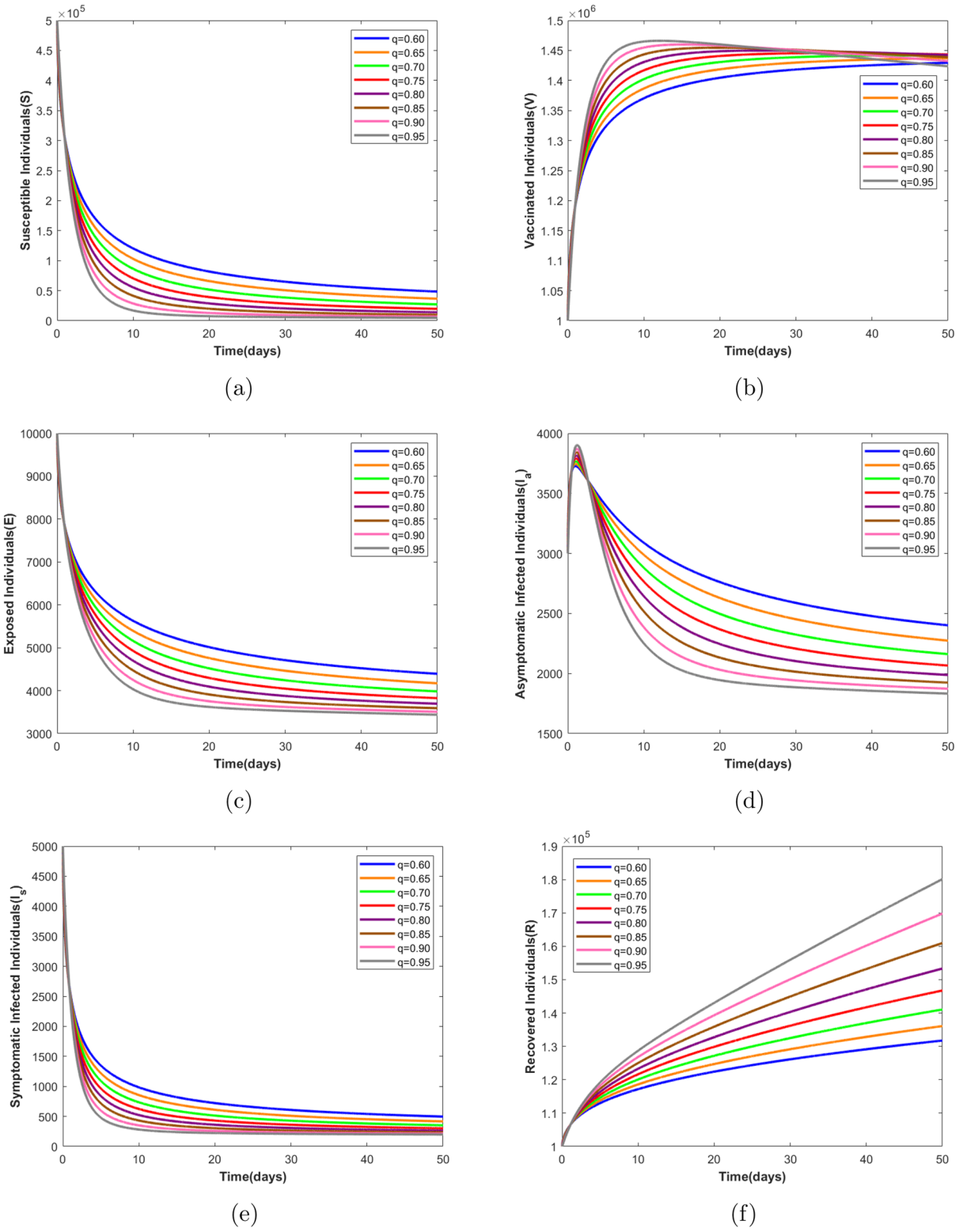

FIG. 1. Numerical simulation of the fractional order model with different values of $q = 0.60, 0.65, 0.70, 0.75, 0.80, 0.85, 0.90, 0.95$. (a) Susceptible individuals, (b) vaccinated individuals, (c) exposed individuals, (d) asymptomatic infected individuals, (e) symptomatic infected individuals, and (f) recovered individuals.

At t_1, we have

$$\|D_{1_n}(t)\| \leq \left[\frac{\chi^{1-q}}{\Gamma(q)} t_1\right]^{n+1} k_1^{n+1} h. \tag{51}$$

As n tends to infinity, $\|D_{1_n}(t)\|$ in (51) converges to zero. Similarly, by taking the limit of $\|D_{i_n}(t)\|$ as n approaches infinity, we find that $\|D_{i_n}(t)\| \to 0$, $i = 2, 3, \ldots, 7$. □

Next, to establish the uniqueness of the solution, we consider an alternative solution, denoted by $S_1, V_1, E_1, I_{a_1}, I_{s_1}, R_1$, and C_1. Hence, we derive the following:

$$S(t) - S_1(t) = \frac{\chi^{1-q}}{\Gamma(q)} \int_0^t (G_1(\varphi, S) - G_1(\varphi, S_1)) d\varphi. \tag{52}$$

Taking norm of (52),

$$\|S(t) - S_1(t)\| = \frac{\chi^{1-q}}{\Gamma(q)} \int_0^t \|(G_1(\varphi, S) - G_1(\varphi, S_1))\| d\varphi. \tag{53}$$

From (41),

$$\|S(t) - S_1(t)\| \leq \frac{\chi^{1-q}}{\Gamma(q)} k_1 \|S - S_{n-1}\| t. \tag{54}$$

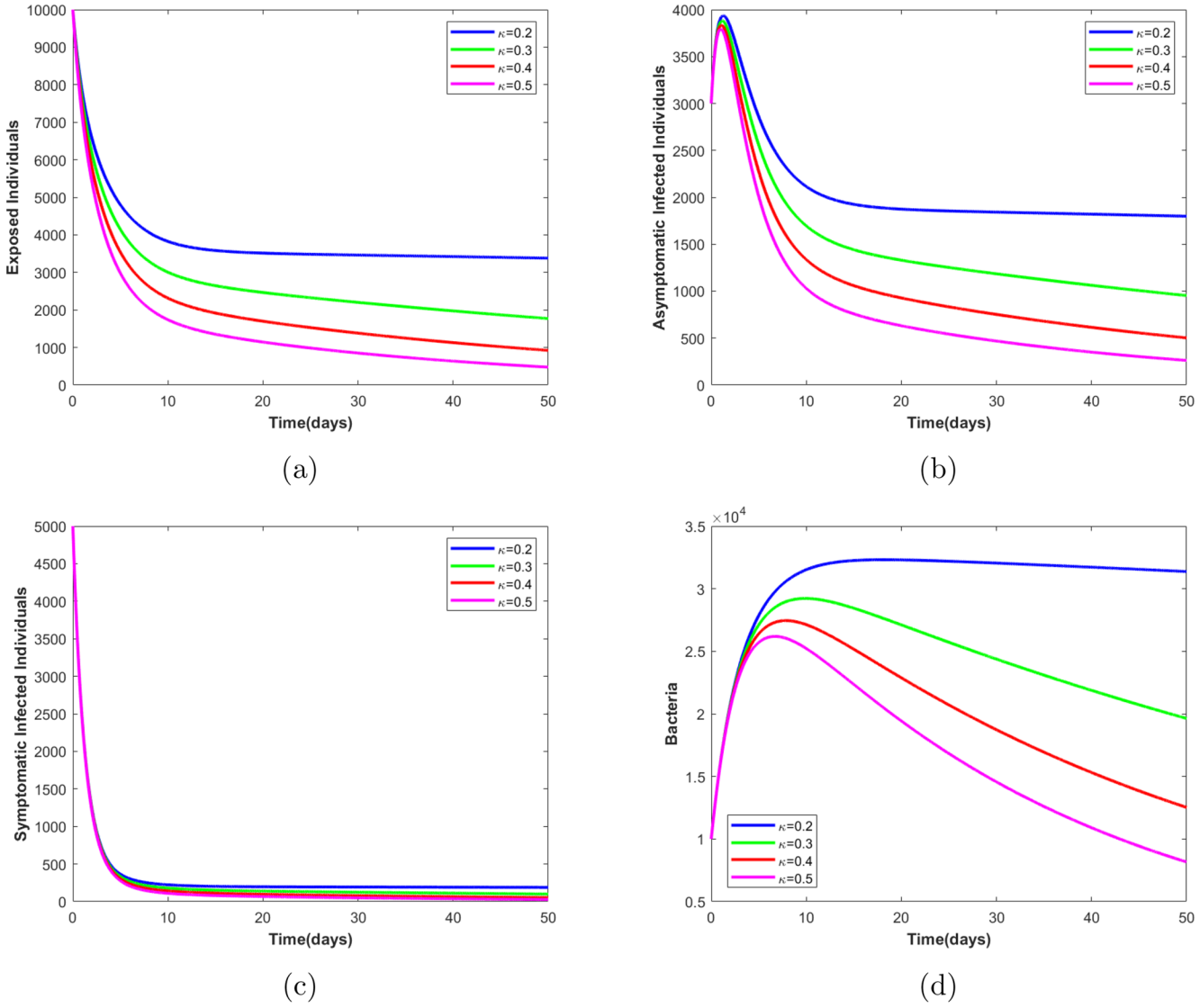

FIG. 2. Simulations describing variations in the number of exposed individuals (a), asymptomatic infected individuals (b), symptomatic infected individuals (c), and the bacterial compartment (d) under different reductions in infectiveness, represented by $\kappa = 0.2, 0.3, 0.4, 0.5$.

Thus,

$$\|S(t) - S_1(t)\|\left(1 - \frac{\chi^{1-q}}{\Gamma(q)}k_1 t\right) \leq 0. \tag{55}$$

Theorem 9. *The solution of the fractional order typhoid fever model (36) is unique if*

$$1 - \frac{\chi^{1-q}}{\Gamma(q)}k_1 t > 0. \tag{56}$$

Proof. Suppose that (56) holds, and then,

$$\|S(t) - S_1(t)\|\left(1 - \frac{\chi^{1-q}}{\Gamma(q)}k_1 t\right) \leq 0.$$

Then, $\|S(t) - S_1(t)\| = 0$. So, we obtain $S(t) = S_1(t)$. Likewise, we can demonstrate equality for V, E, I_a, I_s, R, and C. □

V. NUMERICAL ANALYSIS AND DISCUSSION

In this section, numerical simulations were conducted using the Caputo operator q in accordance with the fractional model (36)

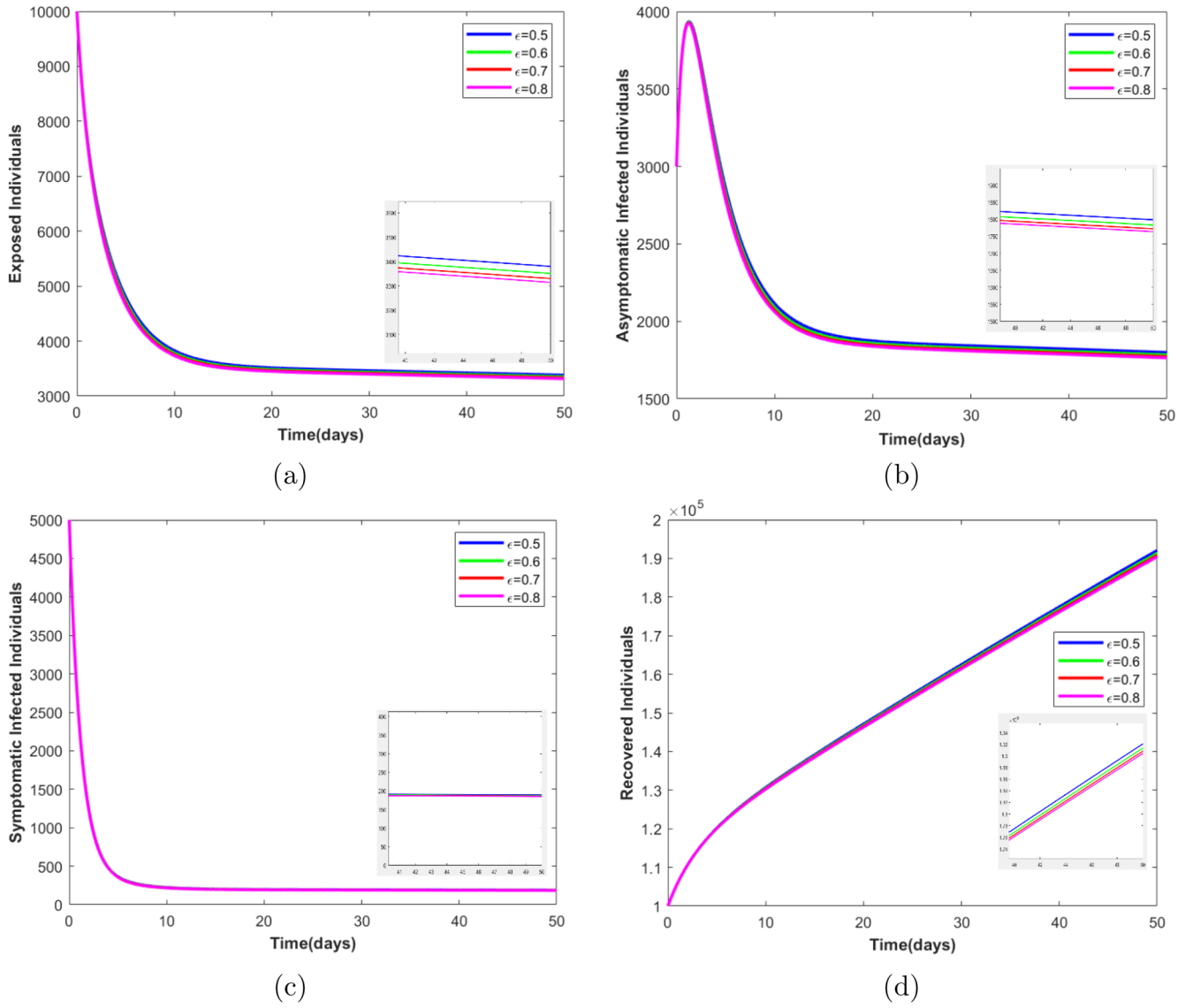

FIG. 3. Simulations describing variations in the number of exposed individuals (a), asymptomatic infected individuals (b), symptomatic infected individuals (c), and recovered individuals (d) under different increments in the vaccination level, represented by $\epsilon = 0.5, 0.6, 0.7, 0.8$.

employing the biological parameter values specified in Table IV. The simulation results showing the variation in the state variables over time are shown in Fig. 1.

Next, we explored the impact of our model parameters, with a focus on the crucial aspects of controlling and preventing typhoid epidemics. Self-sanitation and vaccination interventions were identified as key measures. Subsequently, we analyzed the influence of these interventions on our model.

In Fig. 2, the impact of protective measures, such as practicing safe sanitation, on the exposed, asymptomatic infected, symptomatic infected, and bacterial compartments is shown. Increasing the number of these interventions effectively decreased these populations. Similarly, Fig. 3 illustrates that enhancing vaccination rates reduces the exposed, asymptomatic, and symptomatic infected populations, ultimately leading to a decline in the recovered population. These findings emphasize the critical role of public awareness, particularly in communities susceptible to typhoid fever, as a vital component of comprehensive disease control strategies.

VI. CONCLUSION

In this study, we initially developed a deterministic model for typhoid fever and subsequently transformed it into a fractional-order model using the Caputo derivative. The analysis of the initially deterministic compartmental model presented in Eqs. (2)–(8) reveal two equilibrium points: disease-free equilibrium (DFE) and endemic equilibrium (EE). The global asymptotic stability of the DFE is established when $R_0 < 1$ within the region of attraction $\mathbb{X}$. The fractional model offers a refined perspective on the behavior of the disease, capturing complexities that are not evident in traditional models. Considering these results, our study recommends the implementation of targeted measures by authorities to mitigate the prevalence of typhoid fever. These measures should encompass enforceable vaccination initiatives and policies promoting self-sanitation, representing crucial strategies to curtail the transmission and impact of typhoid fever in the population.

ACKNOWLEDGMENTS

This research was funded by "Petchra Pra Jom Klao Ph.D. Research Scholarship from King Mongkut's University of Technology" under Grant No. 14/2564. The authors are grateful to the editors and reviewers for their thoughtful and insightful comments that improved the manuscript.

AUTHOR DECLARATIONS

Conflict of Interest

The authors have no conflicts to disclose.

Author Contributions

All authors contributed equally to the manuscript and typed it. All the authors have read and agreed to the published version of the manuscript.

Alhassan Ibrahim: Formal analysis (equal); Writing – original draft (equal). **Usa Wannasingha Humphries**: Supervision (equal); Writing – review & editing (equal). **Ibrahim Mohammed**: Conceptualization (equal); Data curation (equal). **Rahat Zarin**: Writing – original draft (equal); Writing – review & editing (equal).

DATA AVAILABILITY

The data that support the findings of this study are available from the corresponding author upon reasonable request.

REFERENCES

[1] J. Wain, R. Hendriksen, M. Mikoleit, K. Keddy, and R. Ochiai, "Typhoid fever," Lancet **385**, 1136 (2015).
[2] WHO, Typhoid, World Health Organization, 2023, https://www.who.int/news-room/fact-sheets/detail/typhoid.
[3] J. J. Muyembe-Tamfum, J. Veyi, M. Kaswa, O. Lunguya, J. Verhaegen, and M. Boelaert, "An outbreak of peritonitis caused by multidrug-resistant *Salmonella Typhi* in Kinshasa, Democratic Republic of Congo," Travel Med. Infect. Dis. **7**(1), 40–43 (2009).
[4] R. Baddam, N. Kumar, K. L. Thong, S. T. Ngoi, C. S. J. Teh, K. P. Yap, and N. Ahmed, "Genetic fine structure of a *Salmonella enterica* serovar Typhi strain associated with the 2005 outbreak of typhoid fever in Kelantan, Malaysia," J. Bacteriol. **194**, 3565 (2012).
[5] E. Kang, A. Crouse, L. Chevallier, S. M. Pontier, A. Alzahrani, N. Silué, F. X. Campbell-Valois, X. Montagutelli, S. Gruenheid, and D. Malo, "Enterobacteria and host resistance to infection," Mamm. Genome **29**, 558–576 (2018).
[6] CDC, Typhoid fever, Centers for Disease Control and Prevention, 2020, www.cdc.gov/typhoid-fever/index.html.
[7] WHO, Diarrhoeal diseases, World Health Organization, 2023, https://web.archive.org/web/20111118000119/http://www.who.int/vaccineresearch/diseases/diarrhoeal/en/index7.html.
[8] R. Milligan, M. Paul, M. Richardson, and A. Neuberger, "Vaccines for preventing typhoid fever," Cochrane Database Syst. Rev. **5**, CD001261 (2018).
[9] H. Abboubakar and R. Racke, "Mathematical modeling, forecasting, and optimal control of typhoid fever transmission dynamics," Chaos, Solitons Fractals **149**, 111074 (2021).
[10] C. B. Acosta-Alonzo, I. V. Erovenko, A. Lancaster, H. Oh, J. Rychtář, and D. Taylor, "High endemic levels of typhoid fever in rural areas of Ghana may stem from optimal voluntary vaccination behaviour," Proc. R. Soc. A **476**(2241), 20200354 (2020).
[11] A. Kailan Suhuyini and B. Seidu, "A mathematical model on the transmission dynamics of typhoid fever with treatment and booster vaccination," Front. Appl. Math. Stat. **9**, 1151270 (2023).
[12] O. J. Peter, M. O. Ibrahim, H. O. Edogbanya, F. A. Oguntolu, K. Oshinubi, A. A. Ibrahim, and J. O. Lawal, "Direct and indirect transmission of typhoid fever model with optimal control," Results Phys. **27**, 104463 (2021).
[13] S. Mushayabasa, "Impact of vaccines of controlling typhoid fever in Kassana-Nankana district of upper east region of Ghana: Insight from a mathematical model," J. Mod. Math. Stat. **5**, 54 (2011).
[14] A. Fraser, M. Paul, E. Goldberg, C. J. Acosta, and L. Leibovici, "Typhoid fever vaccines: Systematic review and meta-analysis of randomised controlled trials," Vaccine **25**(45), 7848–7857 (2007).
[15] A. Awofisayo-Okuyelu, N. McCarthy, I. Mgbakor, and I. Hall, "Incubation period of typhoidal salmonellosis: A systematic review and meta-analysis of outbreaks and experimental studies occurring over the last century," BMC Infect. Dis. **18**, 483 (2018).
[16] H. J. B. Njagarah and F. Nyabadza, "Modeling the impact of rehabilitation, amelioration and relapse on the prevalence of drug epidemics," J. Biol. Syst. **21**(01), 1350001 (2013).

[17]P. Van den Driessche and J. Watmough, "Reproduction numbers and subthreshold endemic equilibria for compartmental models of disease transmission," Math. Biosci. **180**(1–2), 29–48 (2002).
[18]A. Ibrahim, U. W. Humphries, P. S. Ngiamsunthorn, I. A. Baba, S. Qureshi, and A. Khan, "Modeling the dynamics of COVID-19 with real data from Thailand," Sci. Rep. **13**(1), 13082 (2023).
[19]S. S. Musa, A. Yusuf, Z. U. Abdullahi, L. Adamu, U. T. Mustapha, and D. He, "Unravelling the dynamics of Lassa fever transmission with differential infectivity: Modeling analysis and control strategies," Math. Biosci. Eng. **19**, 13114 (2022).
[20]A. Ibrahim, U. W. Humphries, A. Khan, S. Iliyasu Bala, I. A. Baba, and F. A. Rihan, "COVID-19 model with high- and low-risk susceptible population incorporating the effect of vaccines," Vaccines **11**(1), 3 (2022).
[21]C. Castillo-Chavez, Z. Feng, and W. Huang, "On the computation of R_0 and its role on global stability," in *Mathematical Approaches for Emerging and Re-Emerging Infection Diseases: An Introduction*, 125 (Springer, 2002), pp. 31–65.
[22]X. L. Wang, S. Tao, R. W. Dawson, and X. J. Wang, "Uncertainty analysis of parameters for modeling the transfer and fate of benzo(*a*)pyrene in Tianjin wastewater irrigated areas," Chemosphere **55**(4), 525–531 (2004).
[23]I. Ghosh, P. K. Tiwari, and J. Chattopadhyay, "Effect of active case finding on dengue control: Implications from a mathematical model," J. Theor. Biol. **464**, 50–62 (2019).
[24]N. H. Tuan, H. Mohammadi, and S. Rezapour, "A mathematical model for COVID-19 transmission by using the Caputo fractional derivative," Chaos, Solitons Fractals **140**, 110107 (2020).
[25]H. Singh and P. Mahajan, "Analytical modeling of low velocity large mass impact on composite plate including damage evolution," Compos. Struct. **149**, 79–92 (2016).
[26]S. Rezapour, H. Mohammadi, and M. E. Samei, "SEIR epidemic model for COVID-19 transmission by Caputo derivative of fractional order," Adv. Differ. Equations **2020**, 490.
[27]J. M. Mutua, F. B. Wang, and N. K. Vaidya, "Modeling malaria and typhoid fever co-infection dynamics," Math. Biosci. **264**, 128–144 (2015).